Journal of Sound and Vibration (2002) **255**(5), 915–930
doi:10.1006/jsvi.2001.4194, available online at http://www.idealibrary.com on IDEAL®

IDENTIFICATION OF CRACK LOCATION IN VIBRATING BEAMS FROM CHANGES IN NODE POSITIONS

M. Dilena and A. Morassi

Department of Civil Engineering, University of Udine, Via delle Scienze 208, 33100 *Udine, Italy.*
E-mail: antonino.morassi@dic.uniud.it

(*Received* 29 *May* 2001, *and in final form* 28 *August* 2001)

It is known that the effect of a single crack in an axially vibrating thin rod is to cause the nodes of the mode shapes move toward the crack. This paper is an analytical/experimental investigation of the analogous problem for a thin beam in bending vibration. The monotonicity property linking changes in node position and crack location does not hold in the bending case. The analysis of the direct problem, however, shows that the direction by which nodal points move may be useful for predicting damage location. Analytical results agree well with experimental tests performed on cracked steel beams.

1. INTRODUCTION

This paper focuses on detecting a single crack in a beam when damage-induced shifts in the nodes of the mode shapes of the beam in bending vibration are known.

Despite a very extensive literature on damage identification through frequency measurements, see, for instance, references [1–9], very little work has been done on using changes in the nodes of the mode shapes to identify localized damage. In a recent paper, Gladwell and Morassi [10] investigated the effect of a single crack on the nodes of free vibration modes of a thin rod in longitudinal vibration. By simulating damage induced by a spring, it was shown that *nodes move toward the crack*, that is, each node located to the left of the crack in the undamaged configuration moves to the right, and each node on the right of it moves to the left. This means that for every principal mode, which has at least two nodes, there is exactly one neighboring pair of nodes which move toward each other, and the crack is located between them.

The paper [10] left an important question unsolved, namely, the capability to extend this result to cracked beams in bending vibration. Although desirable for the application of diagnostic methods, the existence of a result of this type is all but obvious. In fact, the monotonicity property found in reference [10] is a consequence of the *oscillation and separation theorems* for solutions of the Sturm–Liouville operator governing the axial vibration of a thin rod, see references [11, 12]. General properties of this kind become more involved for the fourth order differential operator of the bending vibrations of a beam, see, for instance, the classical paper by Leighton and Nehari [13]. In particular, on adapting the *Comparison Theorem* 5.1 contained in reference [13], one can show that the bending analogue of the monotonicity property found in reference [10] involves *conjugate points* (associated with one end of the beam) and crack location, that is *conjugate points move toward the crack*. Conjugate points are points of the beam axis given by the intersection of

0022-460X/02/$35.00

two special solutions of the differential operator governing the bending vibrations [13]. Unfortunately, unlike nodal points, conjugate points lack a clear physical interpretation; therefore, since their variations cannot be measured, damage location cannot be deduced. Considering the effect of a crack on the nodal points of flexural modes, the insertion of a crack in some areas of the beam axis was found to cause some nodes to shift away from the damaged area. This effect does not apply to axial modes. Despite no monotonicity property being found to exist between nodes and crack location, a parametrical analysis of the bending problem proved useful to characterize the areas of the beam axis where a crack causes nodes always to shift along the same direction, for varying damage severity, in originally uniform beams with general boundary conditions. In the examined cases, the signs of nodal shifts in the first three/four vibration modes proved essential to assess crack location with good accuracy.

Experimentally, node positions are easier to measure than mode shapes; roughly speaking, they only require the detection of modal component sign, rather than a set of measurements of magnitudes. The dynamic tests performed on slender steel beams with cracks of different severity supported the analytical predictions. This suggests that the proposed method may be used for crack detection in practical situations.

2. CRACK-INDUCED CHANGES IN NODE POSITION

The physical model, which will be thoroughly investigated herein, is a free–free uniform Euler–Bernoulli beam, with an open crack at the cross-section of abscissa s. According to Freund and Herrmann [14], and since only bending vibration is considered, the crack is represented by the insertion of a massless rotational elastic spring at the damaged cross-section. The stiffness K of the spring may be related in a precise way to the geometry of damage as suggested, for example, by Dimarogonas and Paipetis [15]. The eigenpair $(v(\xi), \lambda^4)$ of the undamped bending vibrations of the cracked beam satisfies the following dimensionless boundary value problem:

$$v^{IV}(\xi) = \lambda^4 v(\xi) \quad \text{for } \xi \in (0, \sigma) \cup (\sigma, 1), \tag{1}$$

$$v''(\xi) = 0 = v'''(\xi) \quad \text{at } \xi = 0 \quad \text{and} \quad \xi = 1, \tag{2}$$

where the jump conditions

$$[v(\sigma)] = [v''(\sigma)] = [v'''(\sigma)] = 0, \qquad \mu v''(\sigma) = [v'(\sigma)], \tag{3, 4}$$

hold at the cross-section where the crack occurs. In the equations above, $[\phi(\sigma)] \equiv (\phi(\sigma^+) - \phi(\sigma^-))$ denotes the jump of the function $\phi(\xi)$ at $\xi = \sigma$. The dimensionless quantities ξ, σ, λ^4 and μ are defined as follows:

$$\xi = \frac{x}{L} \quad \text{for } x \in (0, L), \qquad \sigma = \frac{s}{L}, \qquad \lambda^4 = \frac{\rho\omega^2}{EI} L^4, \qquad \mu = \frac{EI}{KL}, \tag{5}$$

where L is the beam length, I represents the moment of inertia of the cross-section, E is the Young's modulus of the material, ρ is the linear mass density and the natural frequency of vibration is denoted by ω. By using standard techniques to solve the boundary value problem (1–4), the eigenvalues λ^4 are the infinite sequence $0 = \lambda_0^4$(*double zero*) $< \lambda_1^4 < \lambda_2^4 < \cdots < \lambda_m^4 < \cdots$ of zeroes of the *characteristic equation*

$$-4 + 4 \cos\lambda \cosh\lambda$$

$$+ \mu\lambda[- \cosh\lambda \sin\lambda - \cosh(1-2\sigma)\lambda \sin\lambda + 2\cosh\sigma\lambda \sin\sigma\lambda$$

$$+ 2\cosh(1-\sigma)\lambda \sin(1-\sigma)\lambda + \cos\lambda \sinh\lambda + \cos(1-2\sigma)\lambda \sinh\lambda$$

$$- 2\cos\sigma\lambda \sinh\sigma\lambda - 2\cos(1-\sigma)\lambda \sinh(1-\sigma)\lambda] = 0. \tag{6}$$

Only strictly positive eigenvalues will be considered hereafter, i.e., the rigid vibrating modes associated to $\lambda_0^4 = 0$ will be omitted. The vibrating mode corresponding to the eigenvalue λ^4 is given by

$$v(\xi) = C_1(\cosh\lambda\xi + \cos\lambda\xi) + D_1(\sinh\lambda\xi + \sin\lambda\xi) \quad \text{for } \xi \in (0, \sigma), \tag{7}$$

$$v(\xi) = C_2(\cosh\lambda(1-\xi) + \cos\lambda(1-\xi)) + D_2(\sinh\lambda(1-\xi) + \sin\lambda(1-\xi)) \quad \text{for } \xi \in (\sigma, 1), \tag{8}$$

where coefficients C_i, D_i, $i = 1, 2$, may be written as

$$C_1 = 1, \tag{9}$$

$$D_1 = \frac{1}{f(\lambda)}[- \cos\sigma\lambda + \cos(1-\sigma)\lambda \cosh\lambda - \cosh\sigma\lambda + \cos\lambda \cosh(1-\sigma)\lambda$$

$$- \sin(1-\sigma)\lambda \sinh\lambda + \sin\lambda \sinh(1-\sigma)\lambda], \tag{10}$$

$$C_2 = \frac{1}{f(\lambda)}[- \cosh\sigma\lambda \sin\lambda + \cosh\lambda \sin\sigma\lambda + \sin(1-\sigma)\lambda$$

$$- \cos\sigma\lambda \sinh\lambda + \cos\lambda \sinh\sigma\lambda + \sinh(1-\sigma)\lambda], \tag{11}$$

$$D_2 = \frac{1}{f(\lambda)}[- \cos(1-\sigma)\lambda + \cos\sigma\lambda \cosh\lambda + \cos\lambda \cosh\sigma\lambda$$

$$- \cosh(1-\sigma)\lambda - \sin\sigma\lambda \sinh\lambda + \sin\lambda \sinh\sigma\lambda], \tag{12}$$

with

$$f(\lambda) = - \cosh(1-\sigma)\lambda \sin\lambda + \sin\sigma\lambda + \cosh\lambda \sin(1-\sigma)\lambda$$

$$- \cos(1-\sigma)\lambda \sinh\lambda + \sinh\sigma\lambda + \cos\lambda \sinh(1-\sigma)\lambda. \tag{13}$$

The undamaged beam corresponds to $K \to \infty$, or, equivalently, to $\mu \to 0$; let $(v_U^{(m)}(\xi), \lambda_{Um}^4)$ be the mth undamaged eigenpair. It is well known that $v_U^{(m)}(\xi)$, $m \geqslant 1$, has $(m+1)$ simple zeros (*nodes*) $\{\xi_i^{(m)}\}_{i=1}^{m+1}$ in the interval $[0, 1]$, e.g., $0 < \xi_1^{(m)} < \cdots < \xi_{m+1}^{(m)} < 1$, see reference [13]; the same property holds true for the mth mode of the damaged beam. For future convenience, one should recall that the bending moment $M_U^{(m)}(\xi) \equiv - EIv_U^{(m)\prime\prime}(\xi)$, $m \geqslant 1$, coincides with the mth vibrating mode of the undamaged beam under clamped–clamped boundary conditions. Then, $M_U^{(m)}(\xi)$ has a double zero at $\xi = 0$ and $\xi = 1$, and it has $(m-1)$ simple zeroes $\{\xi_{iM}^{(m)}\}_{i=1}^{m-1}$ in the interval $(0, 1)$, e.g., $0 < \xi_{1M}^{(m)} < \cdots < \xi_{m-1M}^{(m)} < 1$. Finally, it must be noted that if the crack is located at a cross-section of abscissa σ for which $M_U^{(m)}(\sigma) = 0$, then the related eigenpair is insensitive to damage, that is $(v_U^{(m)}(\xi), \lambda_{Um}^4) \equiv (v^{(m)}(\xi), \lambda_m^4)$. In fact, it can be easily seen that the undamaged vibrating mode identically satisfies the differential equation (1), boundary conditions (2) and jump conditions (3) and (4).

If the exact expression describing the vibration modes of a damaged beam is known, one can parametrically assess the effect of a crack on the nodes of vibration modes when the normalized values of σ position and μ damage severity vary. In particular, Figures 1–5 illustrate the plane domains (σ, μ) corresponding to positive signs (*positive nodal displacement domain*, PNDD, highlighted in Figures 1–5) and negative signs (*negative nodal displacement domain*, NNDD, complementary to the former) of the shift affecting a generic node in the first five vibration modes. Negative domains, NNDD, (and positive PNDD, respectively) correspond to the values of position/damage severity pairs (σ, μ) which, for the node under exam, produce shifts to the left (and to the right, respectively) in the coordinate system elected to represent the points of the beam axis. The variance range for the dimensionless parameter μ in Figures 1–5 is selected so as to include the most significant cases arising in applications, that is, low and medium damage.

It should be recalled that for longitudinal vibrations of a cracked beam, the NNDD of the ith node $\xi_i^{(m)}$ of the mth vibration mode corresponds to the band $\sigma < \xi_i^{(m)}$ of the plane $(\sigma, \mu \equiv EA/KL)$, from which the lines parallel to the axis μ described by equation $\sigma = \xi_{k\,N}^{(m)}$ must be subtracted, where $\xi_{k\,N}^{(m)} < \xi_i^{(m)}$ and $\xi_{k\,N}^{(m)}$ describe the abscissas of the sections where the axial force $N_U^{(m)}(\xi) \equiv EAw_U^{(m)\prime}(\xi)$ is zero, see reference [10]. In the expressions above, EA is the axial rigidity of the beam, L is its length, K is the rigidity of the translational spring used to simulate damage and $w_U^{(m)}(\xi)$ is the axial displacement affecting the section of abscissa ξ in the mth vibration mode of the undamaged beam.

The bending case, as shown in the figures above, is considerably different. In fact, considering a generic node, the plane (σ, μ) is divided into several subsections where boundaries are no more defined by lines parallel to the μ-axis. Despite this, except for some cases like, for instance, the second vibration mode, the boundaries separating the

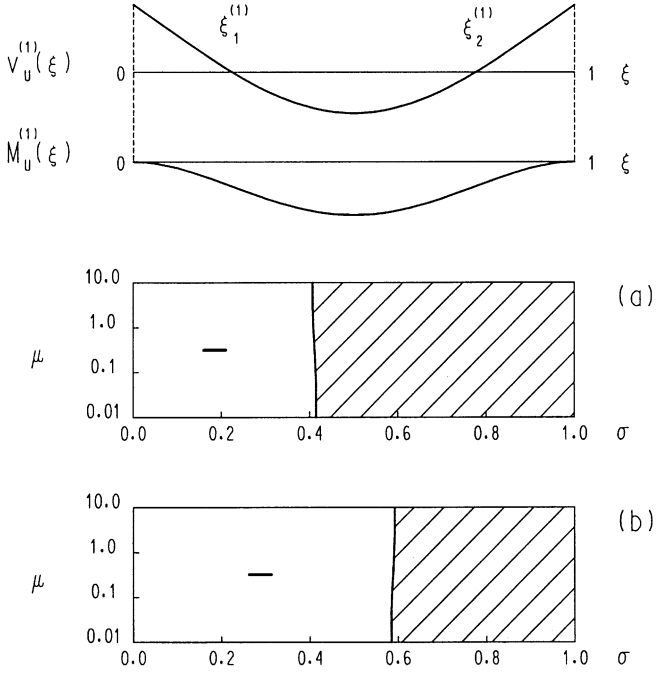

Figure 1. Positive (PNDD, highlighted) and negative (NNDD) nodal displacement domain of the first (a) and second (b) node of the first bending mode.

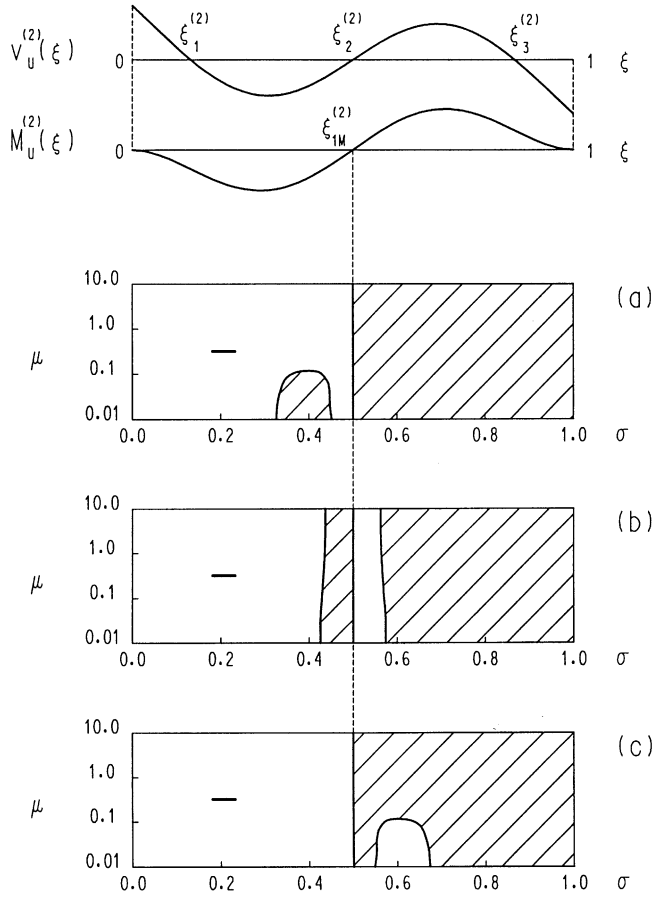

Figure 2. Positive (PNDD, highlighted) and negative (NNDD) nodal displacement domain of the first (a), second (b) and third (c) node of the second bending mode.

subsections belonging to either NNDD or to PNDD are little affected by large variations of μ and are therefore approximately parallel to the μ axis.

A parametrical analysis shows a different behavior in *external nodes* (that is, nodes corresponding to the minimum, $\xi_{\min}^{(m)} \equiv \xi_1^{(m)}$, and maximum, $\xi_{\max}^{(m)} \equiv \xi_{m+1}^{(m)}$, values of the abscissas of the nodal points) and in the remaining *internal nodes.*

Let us concentrate on the modes $m \geqslant 3$ and consider the effects of a crack on the ith internal node, where $2 \leqslant i \leqslant m$. The corresponding NNDD is the union of:

(1) a rectangular band $\sigma < \xi_{i-1\,\mathrm{M}}^{(m)}$, from which a left band adjacent to the line $\sigma = \xi_{i-1\,\mathrm{M}}^{(m)}$ and the bands located alternately to the right and to the left of the lines $\sigma = \xi_{k\,\mathrm{M}}^{(m)}$, where $1 \leqslant k \leqslant (i-2)$, must be subtracted. The latter bands are very narrow along direction σ and only few thousandths of the beam length, see, for example, Figure 6; for this reason, these bands are simply denoted by means of broken vertical lines in Figures 3–5;
(2) a right band adjacent to the line $\sigma = \xi_{i-1\,\mathrm{M}}^{(m)}$;
(3) very narrow bands along direction σ (only few thousandths of the beam length), alternately located to the left and to the right of the lines $\sigma = \xi_{k\,\mathrm{M}}^{(m)}$, where $m-1 \geqslant k \geqslant i$ (broken vertical lines in Figures 3–5).

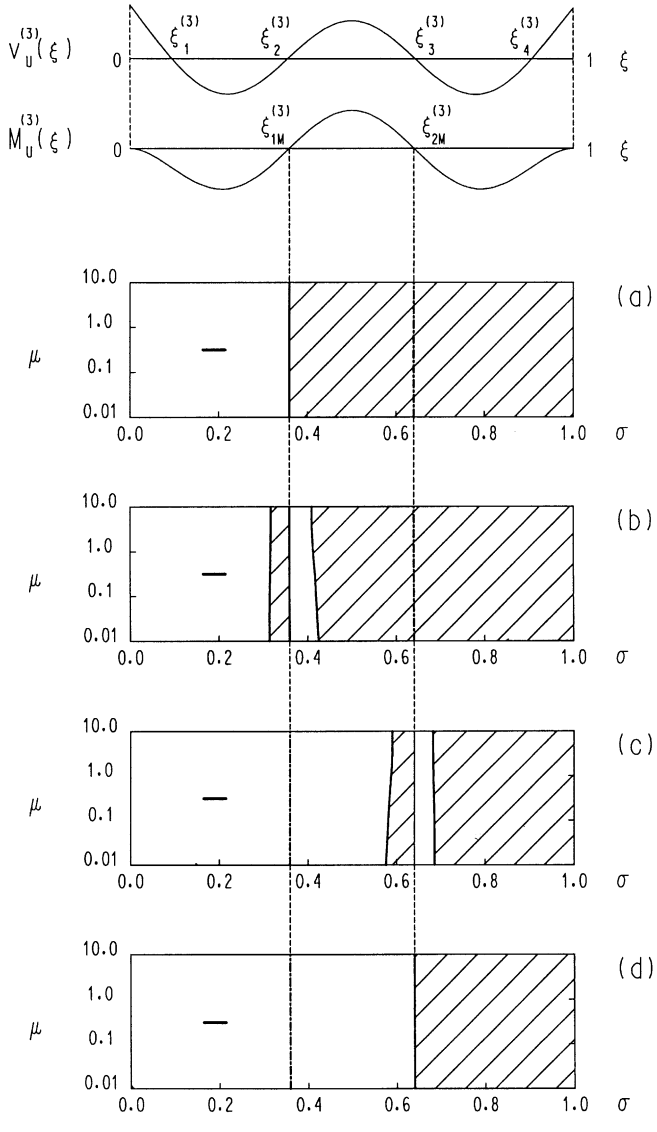

Figure 3. Positive (PNDD, highlighted) and negative (NNDD) nodal displacement domain of the first (a), second (b), third (c) and fourth (d) node of the third bending mode.

The NNDD of the node with $\xi_{\min}^{(m)} \equiv \xi_1^{(m)}$ for the vibration modes where $m \geqslant 3$ is the combination of:

(1) a rectangular band $\sigma < \xi_{1\,\mathrm{M}}^{(m)}$;
(2) very narrow bands along direction σ (only few thousandths of the beam length) alternately located to the left and to the right of the lines $\sigma = \xi_{k\,\mathrm{M}}^{(m)}$, where $m - 1 \geqslant k \geqslant 2$ (broken vertical lines in Figures 3–5).

The NNDD of the node with $\xi_{max}^{(m)} \equiv \xi_{m+1}^{(m)}$ is, for symmetry reasons, complementary to the NNDD associated to the node $\xi_{min}^{(m)} \equiv \xi_1^{(m)}$.

The effects of a crack on the nodes of the first and second vibration modes do not fall in the descriptions above and are distinguished by different characteristics, see Figures 1 and 2.

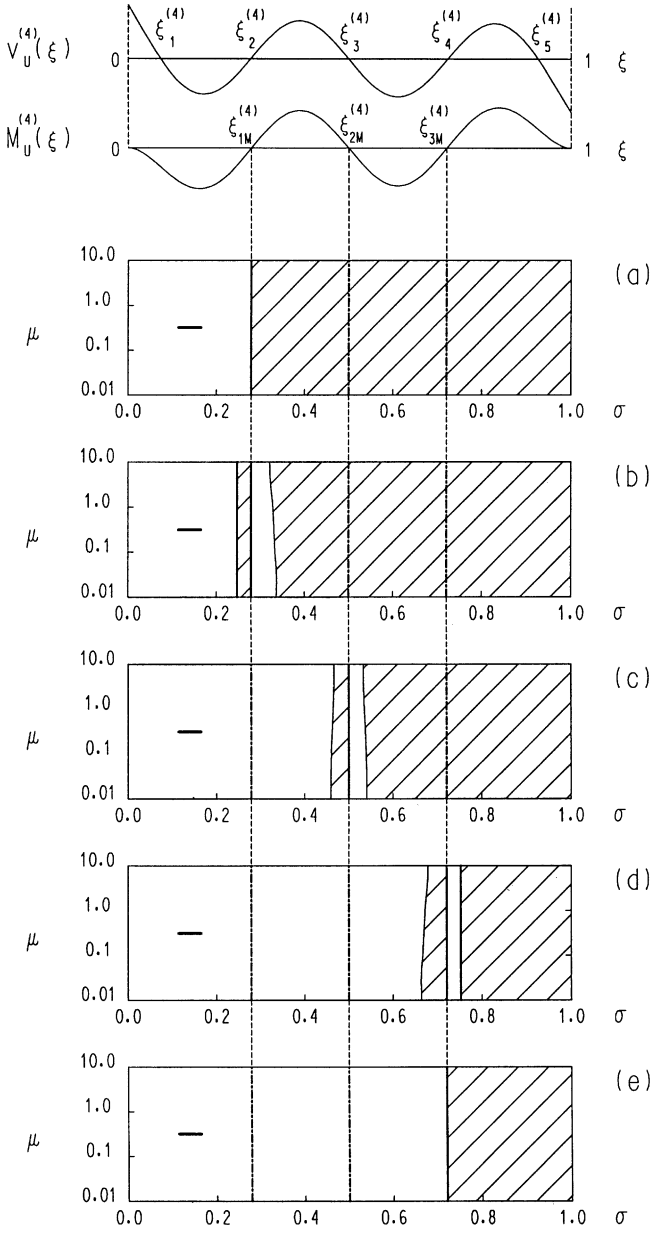

Figure 4. Positive (PNDD, highlighted) and negative (NNDD) nodal displacement domain of the first (a), second (b), third (c), fourth (d) and fifth (e) node of the fourth bending mode.

By way of example, the NNDD of $\xi_1^{(1)}$ is approximately equal to the rectangular band $\sigma < 0{\cdot}4$, although the associated bending moment $M_U^{(1)}(\xi)$ is not zeroed in $(0, 1)$. Concerning the second mode, the NNDD corresponding to an external node is confined by a curve that, for some crack locations, is deeply affected by the value of damage severity.

Results similar to the ones illustrated above were found in uniform beams with different boundary conditions.

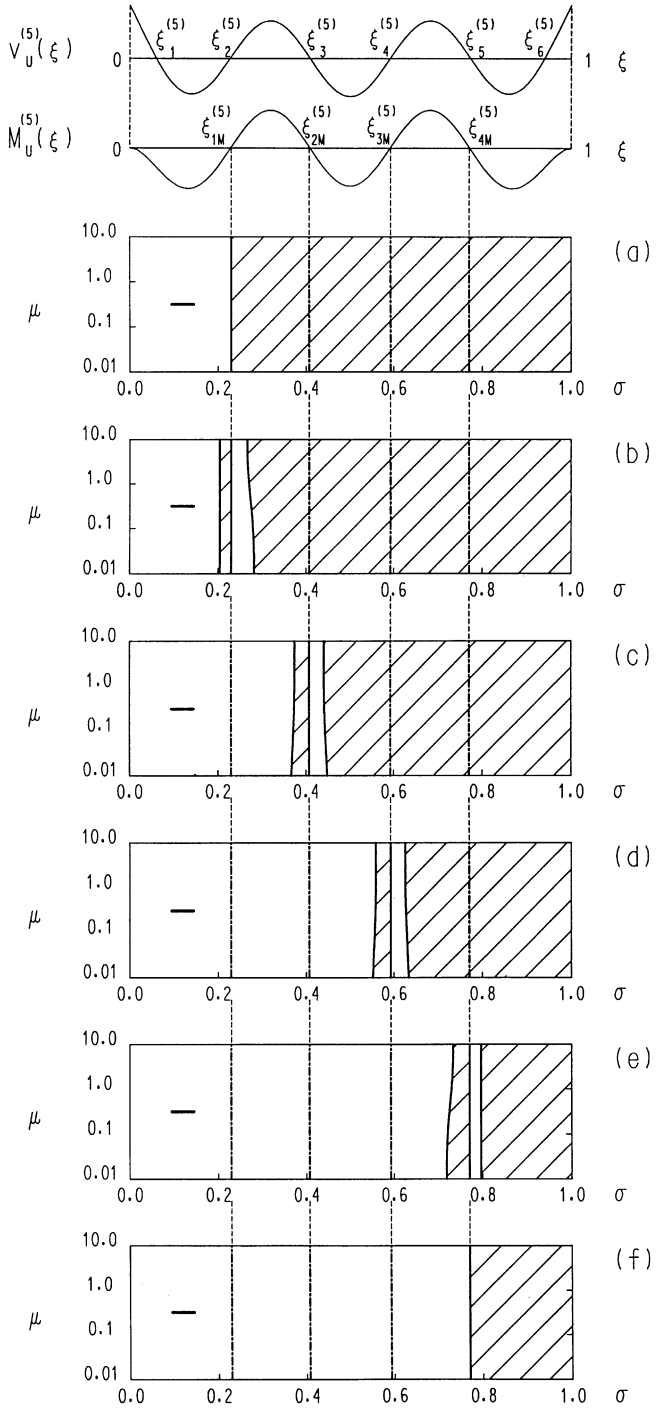

Figure 5. Positive (PNDD, highlighted) and negative (NNDD) nodal displacement domain of the first (a), second (b), third (c), fourth (d), fifth (e) and sixth (f) node of the fifth bending mode.

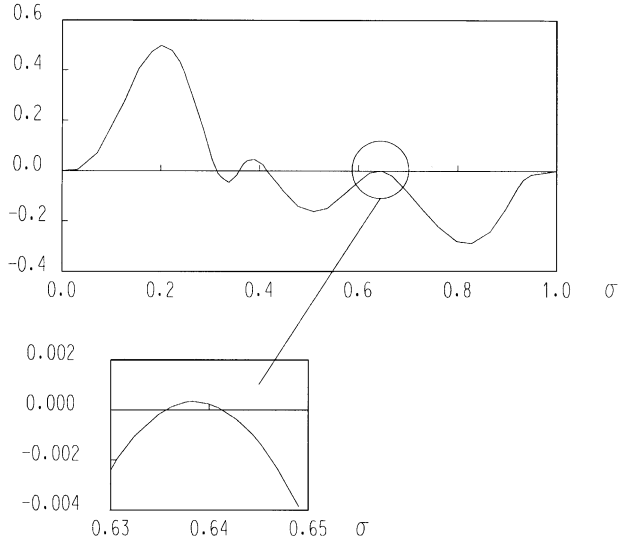

Figure 6. Shift ($\xi_2^{(3)}(damaged) - \xi_2^{(3)}(undamaged)$) of the second node of the third bending mode *versus* crack position ($\mu = 0{\cdot}1$).

3. EXPERIMENTAL RESULTS

Section 2 deals with the description of NNDDs and PNDDs of the nodes of the first modes of a free–free uniform beam in bending vibration. Their practical utility for diagnosis purposes is obvious: tests show the signs of modal shifts, which are then entered in the graphs of Figures 1–5 to identify the areas where damage is likely to be located. A cross-analysis of results for each node of the examined vibration modes and the intersection of the areas where damage is likely to be located can lead to greater accuracy in detection of crack location. Aiming to account for the prospective practical use of the proposed identification technique within the analysis of real cases, the present section is devoted to outlining some applications of experimental character. Some applications to vibrating cracked steel beams under free–free boundary conditions shall be hereinafter considered.

The experimental models are two double T steel beams (T1 and T2) of the series HE100B represented in Figure 7. Each specimen has length $L = 4{\cdot}00$ m and was hung by means of two steel wire ropes fixed at $0{\cdot}80$ m from both ends to simulate free–free boundary conditions. The two beams were damaged by saw-cutting the transversal cross-section at $1{\cdot}80$ m ($\sigma_{T1} = 0{\cdot}45$), $1{\cdot}25$ m ($\sigma_{T2} = 0{\cdot}3125$) from the left end for beam T1 and beam T2 respectively. Two damaged configurations D1 and D2 obtained by introducing cracks of progressive depth were studied, see Figure 7. The scope of the experiment was to measure the shift induced by cracks on the nodes of the low bending vibration modes of the beams.

The technique used to estimate the position of a node is similar to that used in reference [10] and it is based on detecting the phase angle change of the inertance response function between two points of the beam axis including the node. The key notion is that, even though the amplitude of each inertance term is very small near a node, the phase angle is measurable, and should be equal to $+90$ or -90° in the ideal undamped case. The node is located by finding two neighboring points between which the phase angle changes sign. Figure 8 shows a typical inertance term measured near a node of a cracked beam.

Throughout dynamic testing, the flexural response of the beam was measured at one end by a piezoelectric accelerometer PCB 308B02 (weight 72 g). By moving the location of the

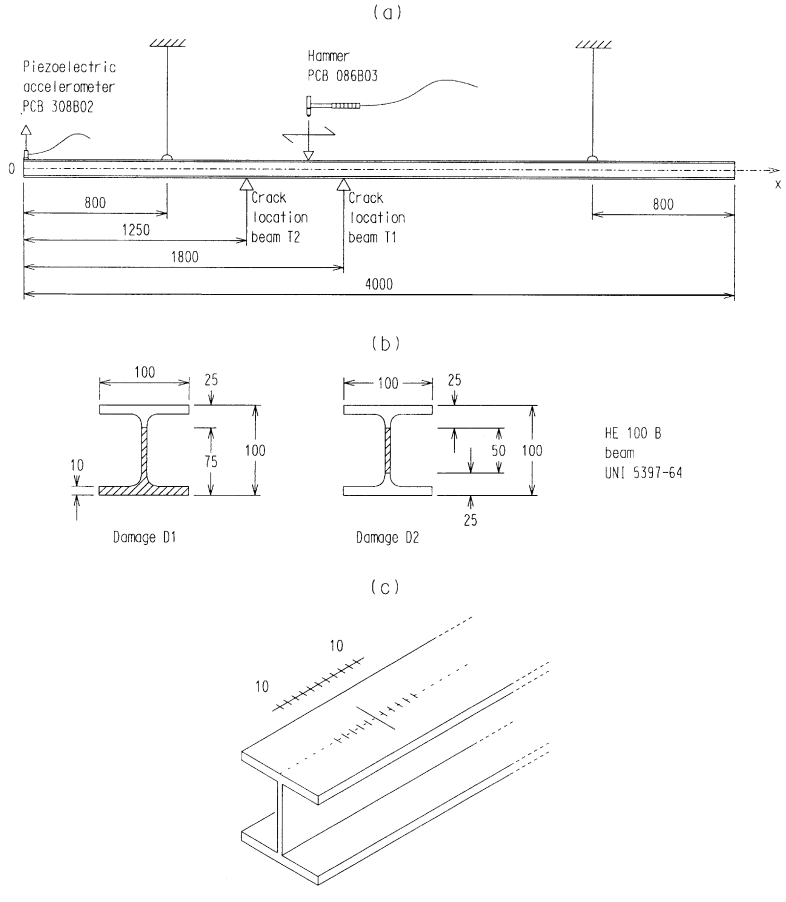

Figure 7. Experimental model (a), damage configurations (b) and measurement grid nears a node position (c). Lengths in mm.

impulse force hammer PCB 086B03 used to excite the specimen, inertance was measured at a grid of points close to an estimated position of each node. The estimate for the undamaged beam was the expected analytical node position. The corresponding initial estimate for the cracked beam was the measured node position for the undamaged beam. This choice was motivated by the observation that the position of a node is a continuous function of damage severity. With the above experimental set-up, each node position was estimated within $\pm 5 \times 10^{-3}$ m.

Tests were run according to an *impulse technique*. The signals were acquired with a sampling frequency of 51·2 KHz by a dynamic analyzer HP 35670A and then decimated in time in order to obtain aliasing free data in the considered frequency range. The input signal was weighted by means of a *force* window, while an *exponential* window was adopted to force to zero the amplitude of the structural response within the acquisition time. Signals were then considered in the frequency domain to measure the relevant frequency response term (inertance). The interpretation of measurements was limited to the first five modes. Throughout the experiments, zoom analysis was performed, with a resolution of 1/16 Hz in the interval ($f_n - 12{\cdot}5$ Hz, $f_n + 12{\cdot}5$ Hz) around each natural frequency f_n. In all cases, each inertance term was evaluated as the mean of five impulsive tests. The measured inertance function for both undamaged and damaged configurations was quite regular and close to

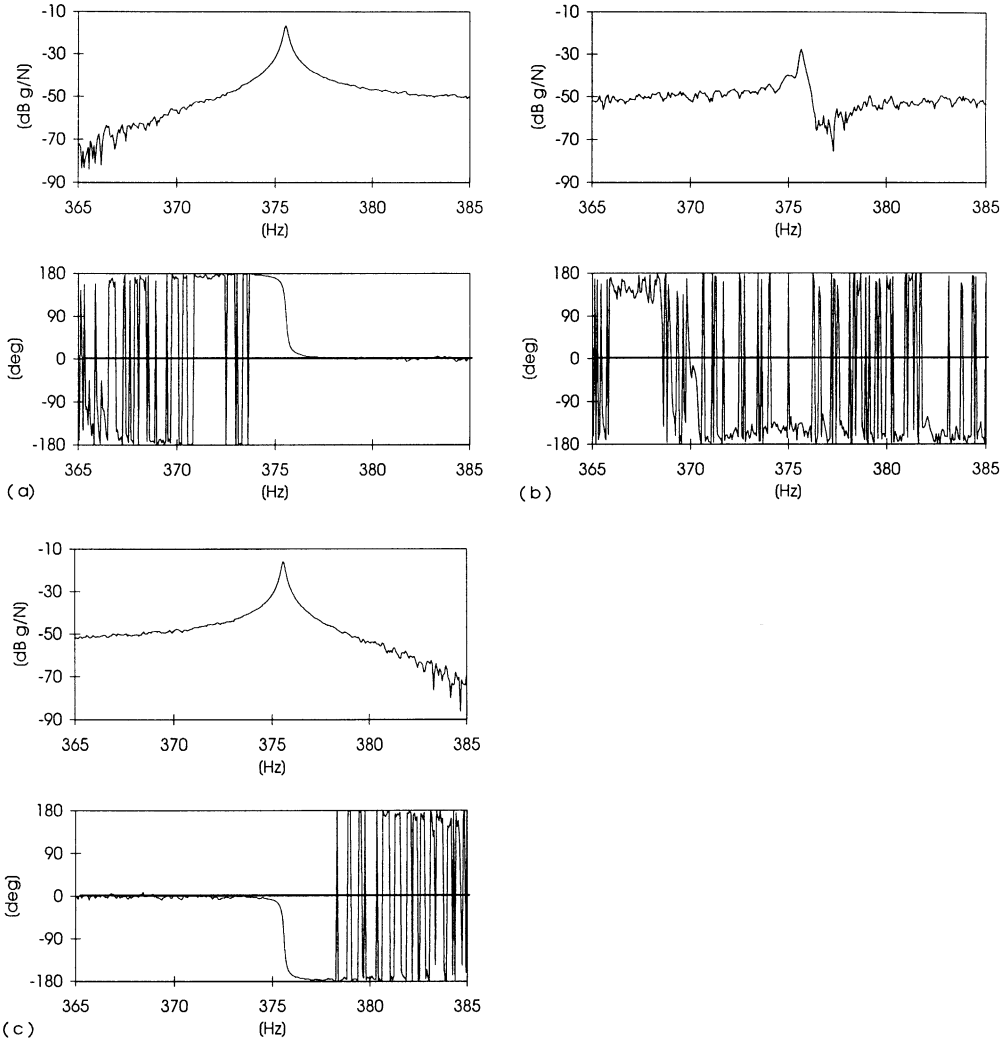

Figure 8. Typical behavior of the inertance near a node of a mode shape (fourth node of the fourth mode, beam T1, damage D1). (a) Just to the left of the node; (b) at the node; (c) just to the right of the node.

that expected for a one-dimensional model of a bending vibrating beam. The well-separated vibration modes and the very small damping effects allowed identifying natural frequencies and the phase angle by means of the single mode technique.

The measurements are summarized in Tables 1 and 2 (node location) and in Tables 5 and 6 (natural frequencies), while Tables 3 and 4 show the experimental node shifts due to the crack.

For the interpretation of dynamic tests on the undamaged configuration, the classical one-dimensional model for bending vibrations of uniform thin beams was adopted. Mass density was evaluated from the measured total mass, while bending stiffness was calculated by taking the measured value as the fundamental frequency of the beam. A comparison between experimental and theoretical frequencies is shown in Tables 5 and 6: agreement is quite good, with percentage errors increasing as the order of the modes rises.

TABLE 1

Experimental and analytical (within parentheses) node locations for beam T1 (lengths in meters). Beam length $L = 4$ m, abscissa of the cracked cross-section $s_{T1} = 1{\cdot}8$ m

State	Mode number	First node	Second node	Third node	Fourth node	Fifth node	Sixth node
Undam.	1	0·905	3·095				
		(0·897)	(3·103)				
	2	0·530	2·000	3·475			
		(0·528)	(2·000)	(3·472)			
	3	0·380	1·430	2·575	3·615		
		(0·378)	(1·423)	(2·577)	(3·622)		
	4	0·305	1·110	2·000	2·885	3·700	
		(0·294)	(1·107)	(2·000)	(2·893)	(3·706)	
	5	0·245	0·915	1·645	2·355	3·085	3·755
		(0·240)	(0·906)	(1·637)	(2·363)	(3·094)	(3·760)
Damage D1	1	0·920	3·045				
		(0·907)	(3·074)				
	2	0·525	2·005	3·465			
		(0·528)	(2·009)	(3·466)			
	3	0·390	1·440	2·535	3·600		
		(0·392)	(1·443)	(2·543)	(3·609)		
	4	0·305	1·125	1·990	2·870	3·695	
		(0·299)	(1·120)	(1·990)	(2·873)	(3·701)	
	5	0·250	0·930	1·645	2·335	3·070	3·750
		(0·244)	(0·922)	(1·642)	(2·342)	(3·079)	(3·756)
Damage D2	1	0·960	2·960				
		(0·925)	(3·022)				
	2	0·510	1·995	3·455			
		(0·526)	(2·018)	(3·458)			
	3	0·410	1·470	2·510	3·590		
		(0·411)	(1·471)	(2·506)	(3·591)		
	4	0·305	1·130	1·980	2·850	3·690	
		(0·305)	(1·130)	(1·977)	(2·853)	(3·696)	
	5	0·255	0·940	1·650	2·325	3·060	3·745
		(0·248)	(0·937)	(1·650)	(2·326)	(3·064)	(3·752)

Measurements on the damaged configuration were interpreted by using the mathematical model discussed in section 2. For each damage configuration, the constant μ was obtained by assuming that position σ of the crack is known and by taking the measured value as the fundamental frequency of the cracked beam. Tables 5 and 6 compare the analytical estimates and the measured values of the first five frequencies: modelling errors are comparable to those of the classical model of an undamaged beam. Tables 1 and 2 show that there is a good agreement between the experimental and theoretical values of node location. It should be noted that, meeting analytical expectations, the insertion of the crack in beam T2 caused the node $\xi_{min}^{(m)}$, $m = 1, 2, 3$, and the second node of the fourth vibration mode to shift away from the damaged section.

Finally, taking into account the results of section 2, Tables 3, 4 and Figures 1–5 can be used for localizing the crack. Regarding beam T1 ($s_{T1} = 0{\cdot}45L$), for example, knowledge of the changed sign of nodes of the first mode only allows locating the crack within the interval $(0{\cdot}4L, 0{\cdot}6L)$. Considering higher modes, the interval of possible damage position is reduced to $(0{\cdot}43L, 0{\cdot}46L)$. By using the same procedure for beam T2 ($s_{T2} = 0{\cdot}3125L$), the crack can

TABLE 2

Experimental and analytical (within parentheses) node locations for beam T2 (lengths in meters). Beam length $L = 4$ m, abscissa of the cracked cross-section $s_{T2} = 1{\cdot}25$ m

State	Mode number	First node	Second node	Third node	Fourth node	Fifth node	Sixth node
Undam.	1	0·910	3·075				
		(0·897)	(3·103)				
	2	0·520	2·000	3·475			
		(0·528)	(2·000)	(3·472)			
	3	0·375	1·425	2·570	3·620		
		(0·378)	(1·423)	(2·577)	(3·622)		
	4	0·295	1·105	1·995	2·890	3·700	
		(0·294)	(1·107)	(2·000)	(2·893)	(3·706)	
	5	0·245	0·910	1·635	2·360	3·090	3·755
		(0·240)	(0·906)	(1·637)	(2·363)	(3·094)	(3·760)
Damage D1	1	0·860	3·050				
		(0·863)	(3·076)				
	2	0·510	1·910	3·440			
		(0·523)	(1·919)	(3·442)			
	3	0·370	1·420	2·550	3·615		
		(0·376)	(1·422)	(2·561)	(3·618)		
	4	0·300	1·100	1·980	2·875	3·695	
		(0·298)	(1·097)	(1·984)	(2·882)	(3·703)	
	5	0·260	0·920	1·560	2·290	3·055	3·740
		(0·251)	(0·921)	(1·566)	(2·300)	(3·060)	(3·750)
Damage D2	1	0·815	2·945				
		(0·813)	(3·004)				
	2	0·485	1·800	3·395			
		(0·494)	(1·802)	(3·392)			
	3	0·370	1·415	2·540	3·605		
		(0·372)	(1·418)	(2·544)	(3·614)		
	4	0·305	1·095	1·965	2·865	3·695	
		(0·304)	(1·095)	(1·964)	(2·867)	(3·699)	
	5	0·265	0·930	1·515	2·245	3·030	3·740
		(0·262)	(0·931)	(1·508)	(2·240)	(3·027)	(3·742)

be located within the interval (0·28L, 0·32L). Damage severity and the specimen features were probably decisive in successful identification; with less severe damage, the sensitivity of the problem to data accuracy may become important.

4. CONCLUSIONS

This paper has been focused on detecting a single crack when damage-induced shifts in the nodes of the mode shapes of a beam in bending vibration are known. It was shown how the direction by which nodal points shift may be used to estimate the location of damage. Analytical results agree well with experimental tests performed on cracked steel beams. This suggests that it may be possible to use the method in practical situations including, in perspective, more complex vibrating systems and less restrictive classes of damages. The present results represent the first step of a line of research on the damage-induced changes in the null set of eigenfunctions of vibrating systems. In subsequent papers, we plan to extend

TABLE 3

Experimental and analytical (within parentheses) node shifts due to the crack for beam T1. Shifts $\Delta\xi_i^{(m)}$ of the ith node of the mth mode: $\Delta\xi_i^{(m)} = \xi_{iD}^{(m)} - \xi_{iU}^{(m)}$ (lengths in meters)

Damage	Mode number	First node shift	Second node shift	Third node shift	Fourth node shift	Fifth node shift	Sixth node shift
D1	1	0·015	− 0·050				
		(0·011)	(− 0·030)				
	2	− 0·005	0·005	− 0·010			
		(0·000)	(0·009)	(− 0·005)			
	3	0·010	0·010	− 0·040	− 0·015		
		(0·014)	(0·020)	(− 0·034)	(− 0·013)		
	4	0·000	0·015	− 0·010	− 0·015	− 0·005	
		(0·005)	(0·013)	(− 0·010)	(− 0·019)	(− 0·005)	
	5	0·005	0·015	0·000	− 0·020	− 0·015	− 0·005
		(0·004)	(0·016)	(0·005)	(− 0·021)	(− 0·015)	(− 0·004)
D2	1	0·055	− 0·135				
		(0·028)	(− 0·081)				
	2	− 0·020	− 0·005	− 0·020			
		(− 0·003)	(0·018)	(− 0·014)			
	3	0·030	0·040	− 0·065	− 0·025		
		(0·033)	(0·048)	(− 0·071)	(− 0·031)		
	4	0·000	0·020	− 0·020	− 0·045	− 0·010	
		(0·011)	(0·023)	(− 0·023)	(− 0·040)	(− 0·010)	
	5	0·010	0·025	0·005	− 0·030	− 0·025	− 0·010
		(0·008)	(0·032)	(0·014)	(− 0·038)	(− 0·030)	(− 0·008)

TABLE 4

Experimental and analytical (within parentheses) node shifts due to the crack for beam T2. Shifts $\Delta\xi_i^{(m)}$ of the ith node of the mth mode: $\Delta\xi_i^{(m)} = \xi_{iD}^{(m)} - \xi_{iU}^{(m)}$ (lengths in meters)

Damage	Mode number	First node shift	Second node shift	Third node shift	Fourth node shift	Fifth node shft	Sixth node shift
D1	1	− 0·050	− 0·025				
		(− 0·034)	(− 0·027)				
	2	− 0·010	− 0·090	− 0·035			
		(− 0·005)	(− 0·081)	(− 0·030)			
	3	− 0·005	− 0·005	− 0·020	− 0·005		
		(− 0·002)	(− 0·001)	(− 0·015)	(− 0·004)		
	4	0·005	− 0·005	− 0·015	− 0·015	− 0·005	
		(0·004)	(− 0·010)	(− 0·016)	(− 0·011)	(− 0·003)	
	5	0·015	0·010	− 0·075	− 0·070	− 0·035	− 0·015
		(0·011)	(0·016)	(− 0·070)	(− 0·064)	(− 0·035)	(− 0·009)
D2	1	− 0·095	− 0·130				
		(− 0·083)	(− 0·099)				
	2	− 0·035	− 0·200	− 0·080			
		(− 0·035)	(− 0·198)	(− 0·080)			
	3	− 0·005	− 0·010	− 0·030	− 0·015		
		(− 0·006)	(− 0·005)	(− 0·033)	(− 0·008)		
	4	0·010	− 0·010	− 0·030	− 0·025	− 0·005	
		(0·010)	(− 0·015)	(− 0·036)	(− 0·026)	(− 0·007)	
	5	0·020	0·020	− 0·120	− 0·115	− 0·060	− 0·015
		(0·021)	(0·025)	(− 0·128)	(− 0·123)	(− 0·067)	(− 0·018)

TABLE 5

Experimental and analytical frequencies f_m of beam T1. Abscissa of the cracked cross-section $s_{T1} = 1{\cdot}8$ m. (1) $EI = 9{\cdot}5888 \times 10^5$ N m^2, $\rho = 20{\cdot}775$ kg/m, $L = 4{\cdot}0$ m. (2) $K = 2{\cdot}058 \times 10^6$ N m/rad ($\mu = 0{\cdot}116$). (3) $K = 4{\cdot}501 \times 10^5$ N m/rad ($\mu = 0{\cdot}533$). Frequency values in Hz. $\Delta f_m\% = (f_m\,(model) - f_m\,(exp.))/(f_m\,(exp.)) \times 100$

	Undamaged (1)			Damage D1 (2)			Damage D2 (3)		
f_m	Exp.	Model	$\Delta f_m\%$	Exp.	Model	$\Delta f_m\%$	Exp.	Model	$\Delta f_m\%$
f_1	47·813	47·813	0·0	42·188	42·188	0·0	31·375	31·375	0·0
f_2	129·375	131·797	1·8	127·375	129·927	2·0	124·438	127·028	2·1
f_3	245·188	258·375	5·4	231·813	242·745	4·7	214·750	223·518	4·1
f_4	387·563	427·107	10·2	375·625	413·298	10·0	365·625	399·607	9·3
f_5	551·063	638·024	15·8	531·125	617·543	16·3	523·313	598·279	14·3

TABLE 6

Experimental and analytical frequencies f_m of beam T2. Abscissa of the cracked cross-section $s_{T2} = 1{\cdot}25$ m. (1) $EI = 9{\cdot}5137 \times 10^5$ N m^2, $\rho = 20{\cdot}775$ kg/m, $L = 4{\cdot}0$ m. (2) $K = 1{\cdot}983 \times 10^6$ N m/rad ($\mu = 0{\cdot}120$). (3) $K = 4{\cdot}120 \times 10^5$ N m/rad ($\mu = 0{\cdot}577$). Frequency values in Hz. $\Delta f_m\% = (f_m\,(model) - f_m\,(exp.))/(f_m\,(exp.)) \times 100$

	Undamaged (1)			Damage D1 (2)			Damage D2 (3)		
f_m	Exp.	Model	$\Delta f_m\%$	Exp.	Model	$\Delta f_m\%$	Exp.	Model	$\Delta f_m\%$
f_1	47·625	47·625	0·0	44·125	44·125	0·0	34·938	34·938	0·0
f_2	129·250	131·280	1·6	116·563	118·363	1·6	100·375	101·121	0·7
f_3	245·000	257·362	5·1	240·125	252·255	5·1	235·125	246·542	4·9
f_4	387·125	425·432	9·9	380·813	417·279	9·6	373·625	406·368	8·8
f_5	550·375	635·522	15·5	511·563	589·495	15·2	491·375	551·066	12·2

the proposed technique to one-dimensional vibrating systems with diffused cracking and to two-dimensional systems with localized defects, such as plates and shells with holes or line cracks.

REFERENCES

1. R. D. ADAMS, P. CAWLEY, C. J. PYE and B. J. STONE 1978 *Journal of Mechanical Engineering Science* **20**, 93–100. A vibration technique for non-destructively assessing the integrity of structures.
2. P. F. RIZOS, N. ASPRAGATHOS and A. D. DIMAROGONAS 1990 *Journal of Sound and Vibration* **138**, 381–388. Identification of crack location and magnitude in a cantilever beam from the vibration modes.
3. G. HEARN and R. B. TESTA 1991 *American Society of Civil Engineers, Journal of Structural Engineering* **117**, 3042–3063. Modal analysis for damage detection in structures.
4. R. Y. LIANG, J. HU and F. CHOY 1992 *American Society of Civil Engineers, Journal of Engineering Mechanics* **118**, 384–396. Theoretical study of crack-induced eigenfrequency changes on beam structures.
5. Y. NARKIS 1994 *Journal of Sound and Vibration* **172**, 549–558. Identification of crack location in vibrating simply supported beams.

6. C. DAVINI, A. MORASSI and N. ROVERE 1995 *Journal of Sound and Vibration* **179**, 513–527. Modal analysis of notched bars: tests and comments on the sensitivity of an identification technique.
7. F. VESTRONI and D. CAPECCHI 1996 *Journal of Vibration and Control* **2**, 69–86. Damage evaluation in cracked vibrating beams using experimental frequencies and finite element models.
8. R. RUOTOLO and C. SURACE 1997 *Journal of Sound and Vibration* **206**, 567–588. Damage assessment of multiple cracked beams: numerical results and experimental validation.
9. A. MORASSI 2001 *Journal of Sound and Vibration* **242**, 577–596. Identification of a crack in a rod based on changes in a pair of natural frequencies.
10. G. M. L. GLADWELL and A. MORASSI 1999 *Inverse Problems in Engineering* **7**, 215–233. Estimating damage in a rod from changes in node positions.
11. C. STURM 1836 *Journal de Mathématique* **1**, 106–186. Sur les équations differentielle linéares du second ordre.
12. J. LIOUVILLE 1836 *Journal de Mathématique* **1**, 253–265. Mémoire sur le développement des fonctions au parites de fonctions en séries dont les divers termes sont assujettis à satisfaire à une même équation differentielle du second ordre contenant un paramètre variable; 1837 *Journal de Mathématique* **2**, 16–35 and 418–436.
13. W. LEIGHTON and Z. NEHARI 1958 *Transactions of the American Mathematical Society* **89**, 325–377. On the oscillation of solutions of self-adjoint linear differential equations of the fourth order.
14. L. B. FREUND and G. HERRMANN 1976 *Journal of Applied Mechanics* **76-APM-15**, 112–116. Dynamic fracture of a beam or plate in plane bending.
15. A. D. DIMAROGONAS and S. A. PAIPETIS 1983 *Analytical Methods in Rotor Dynamics*, London: Applied Science.